

Halogen discharge on graphite electrodes from silver halide solid electrolytes

D. O. RALEIGH

Science Center, Rockwell International, Thousand Oaks, California 91360

Received 12 February 1974

Halogen ion discharge from the solid electrolytes AgI, AgBr, and $2\text{Me}_4\text{NI} \cdot 13\text{AgI}$ on pressed-powder graphite electrodes at room temperature was examined by cyclic voltammetry on Ag|AgX|C solid state cells. Iodine discharge from AgI occurs rapidly, reversibly, and with a moderate 'undervoltage' ascribable to iodine monolayer buildup. Bromine discharge from AgBr is strongly irreversible and was seen to occur in two stages; a small, permanently saturable discharge attributed to direct formation of bromine-graphite 'residue' compounds, and a steady-state main discharge attributed to formation and fast diffusion of bromine in interlamellar graphite compounds. Iodine discharge from $2\text{Me}_4\text{NI} \cdot 13\text{AgI}$ appears to occur via the formation of Me_4NI_3 . On continuous 0–500 mV voltammetric cycling, incomplete electrolyte recombination leads first to a new iodine discharge reaction and finally to cessation of Faradaic activity.

1. Introduction

With the developing interest in solid-state batteries and fuel cells, Faradaic reactions in solid-electrolyte cell systems are receiving increasing attention [1]. We recently reported the results of room temperature capacitance studies [2] on silver halide-graphite interfaces in pressed-powder cells Ag|AgX|C. In the course of this work, a series of cyclic voltammograms were carried out to investigate the halogen-ion discharge characteristics on graphite as a matter of general interest. The electrolytes AgI, AgBr, and the highly conductive [3] composition $2\text{Me}_4\text{NI} \cdot 13\text{AgI}$ were studied. The results showed interesting distinctions in behaviour, both as a function of the halogen ion and the electrolyte from which discharged, and are reported herein.

2. Experimental

1/4 in diameter Ag|AgX|C pressed-powder cells, with a 0.010 in Ag wire reference electrode embedded in the electrolyte, were prepared as described previously [2, 4]. 5N grades of finely (–325 mesh) powdered Ag, AgI, and AgBr were used, and spectroscopic graphite powder. A sample of $2\text{Me}_4\text{NI} \cdot 13\text{AgI}$, prepared as described previously

[3], was obtained from Dr B.B. Owens. All measurements were made in the ambient laboratory atmosphere, with the cell lightly springloaded between 1/4 in metal rods in a Micarta cell holder. A polarizing d.c. bias of 0.25 V was placed on the cell as a starting potential, and voltage sweep studies commenced after the steady-state cell current had settled to $\lesssim 1$ nA. Cyclic voltammetric sweeps were carried out with a standard potentiostatic arrangement, generally at 74 mV s^{-1} , employing reference electrode feedback via a voltage follower. Resistance compensation was not used. The results reported were observed in several cells of each electrolyte type.

3. Results and discussion

3.1. Silver iodide cells

Fig. 1 shows voltammetric loops for an Ag|AgI|C cell, over the indicated range of graphite electrode voltages anodic to the Ag|AgI reference potential. Voltage sweeps in the range 0–450 mV showed only capacitative charging current, with a nearly voltage-independent capacitance for the AgI|C interface as reported previously [2] from potential-step chronocoulometric studies. At about 200 mV below the standard potential (687 mV) for the

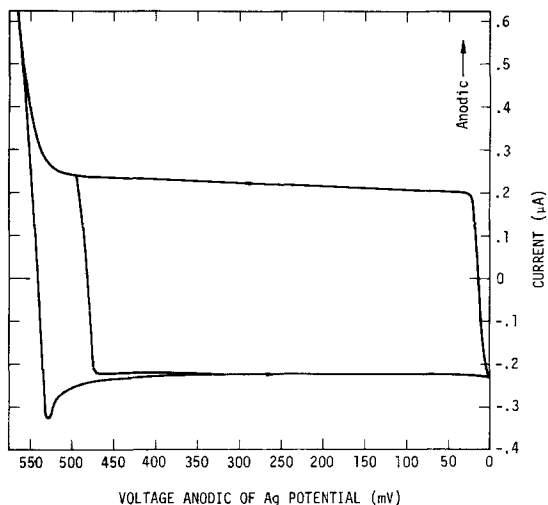
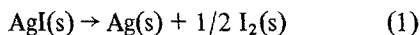


Fig. 1. Cyclic voltammograms, graphite electrode on AgI, 495 and 568 mV anodic limits. Sweep rate 74 mV s^{-1} .

decomposition reaction [5]



I^- discharge appears to commence. At a $\sim 50 \text{ mV}$ more anodic potential, the oxidation current increases rapidly. On sweep reversal, re-reduction appears to occur fairly quickly.

Studies by Connor and co-workers [6] indicate that iodine is reversibly adsorbed on graphite below 200°C , with full monolayer coverage at unit iodine activity. Formation of an adsorbed partial monolayer might then explain the onset of appreciable iodine discharge, well below the standard state potential. A rough estimate which indicates this can be deduced as follows:

From Connor *et al.* the surface area of reversibly adsorbed iodine in a full monolayer is 15.6 \AA^2 , corresponding to a coverage of $6.4 \times 10^{14} \text{ I atoms cm}^{-2}$. Then, assuming monatomic adsorption and an ideal iodine activity-coverage relationship, the maximum partial monolayer concentration at a voltage V below the standard state potential is this value multiplied by $\exp(-FV/RT)$. If for instance, we take $V = 127 \text{ mV}$ (0.56 V on Fig. 1), the expected maximum concentration would be $4.5 \times 10^{12} \text{ I atoms cm}^{-2}$, $\approx 0.73 \text{ } \mu\text{coul cm}^{-2}$ in terms of the associated Faradaic charge transfer. Integration of the charge transfer out to 0.56 V on Fig. 1 in excess of the double layer charging gives $0.17 \text{ } \mu\text{coul cm}^{-2}$. Thus, an ideal-solution partial-monolayer model can accommodate the observed

degree of discharge, indicating the reasonableness of a purely physical adsorption process.

In summary, iodine discharge on graphite from the solid electrolyte AgI at room temperature appears to occur rapidly, reversibly, and in terms of a purely physical adsorption process on the graphite. If, as we suggested in an earlier article [2], AgI|C interfaces contain an interfacial layer of adsorbed anions, then I^- discharge and I monolayer build-up should indeed be rapid, since it would involve simply electron transfer from *in situ* ions, rather than ion motion as well.

3.2. Silver bromide cells

Bromine discharge on graphite from solid AgBr differs qualitatively from that of iodine in many respects. Fig. 2 shows the result of about 20 successive voltammetric sweeps on an Ag|AgBr|C cell in the range 0–500 mV anodic to Ag. As in the

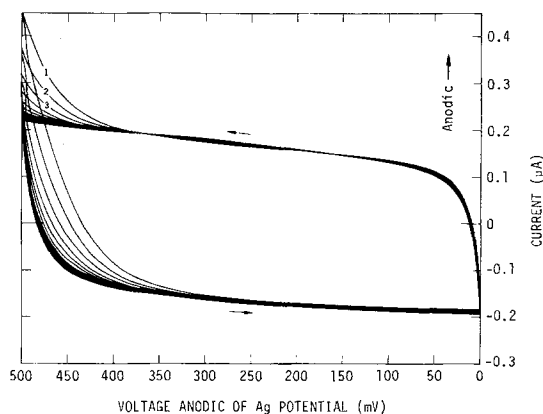


Fig. 2. Cyclic voltammogram sequence, new graphite electrode on AgBr, sweep rate 74 mV s^{-1} .

case of AgI, the loops indicate predominant capacitive charging over most of the voltage range, with the less rectangular loop shape resulting from the larger RC time constant of the more resistive AgBr electrolyte. In distinction, however,

- (1) apparent anionic discharge actually starts $\sim 100 \text{ mV}$ lower than for AgI, despite the higher standard state decomposition potential (0.994 V) for AgBr [7];
- (2) a Faradaic saturation process appears to take place, with repeated sweeps finally resulting in a purely capacitive loop shape;

- (3) the assumed bromine oxidation process appears totally irreversible. The observed Faradaic currents are anodic with respect to the final capacitance loop in both the anodic and cathodic sweep directions. No net cathodic currents are observed.

Several other loop characteristics are of interest:

- (4) The loop shape progression was unaffected by sweep interruptions (in which the voltage was returned to the 0.25 V midpoint) of up to several hours. The progression simply resumed where it had left off.
- (5) If a sweep was stopped at the 0.50 V anodic limit and the voltage held at this value for, e.g. 20 s, the current drifted downward and, on resuming sweeping, the next sweep showed noticeably further progression towards the final capacitance loop shape.
- (6) Once the final loop shape was reached, repeat sweeps showed no further Faradaic effects, even after disconnecting the cell from voltage for several months. Moreover, extending the anodic sweep limit on such cells to as high as 700 mV showed no anodic currents.

These characteristics indicate a totally irreversible oxidation process, in which the product formed stays permanently at the interface, blocking further discharge. The presence of an accidental Faradaic impurity seemed unlikely because of the absence of this effect in the AgI cells, in AgBr cells with platinum electrodes [2] (not otherwise discussed here), and because of the difficulty in imagining any particular impurity in either the graphite or the AgBr that would act in the observed fashion.

Bromine is known to form intercalation compounds in graphite at room temperatures [8, 9], while iodine does not [6, 10]. C_8Br is the most bromine-rich of a series of compounds of the general formula $C_{4n}Br$. Whilst such compounds are readily decomposed by evacuation, heating, or cathodic reduction, a small fraction of the bromine (3–10%) is stubbornly retained. For instance, Hennig [11] reported 92% retention of such residual bromine after heating for 2 days at 350°C. This bromine has been identified with so-called 'residue compounds' [10], in which it appears to be tightly bonded at specific

imperfections in the graphite hexagonal network [10, 12, 13].

Several factors suggest that residue compound formation is involved in the present case. Graphical integration of the net anodic currents in Fig. 2 (with respect to the final capacitance loop) for a sufficient number of cycles, leads to an estimated total Faradaic charge transfer of about $0.85 \mu\text{Coul cm}^{-2}$ at saturation. Since a high degree of *c*-axis orientation exists in the pressed-powder graphite electrode [2], one may assume the carbon-atom density at the interface is roughly that obtaining in the graphite *c*-axis plane. On this basis, the apparent C:Br ratio for the discharged bromine is about 800:1. Thus, a quite small fraction of the electrode area is involved. Further, the considerable 'undervoltage' for discharge of this limited amount of bromine and the extreme irreversibility are in line with the known stability of the residue compounds, both thermal and electrochemical [13].

To see if cyclic voltammetric sweeps to more anodic potentials would result in a well-defined anodic peak for the presumed residue compound formation, sweeps were carried out to 700 mV anodic of Ag|AgBr on freshly prepared cells at a threefold reduced sweep speed. Fig. 3 shows a typical result, showing four successive sweeps and

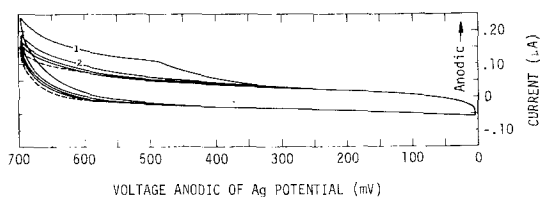


Fig. 3. Cyclic voltammogram sequence, new graphite electrode on AgBr, sweep rate 22 mV s^{-1} . Dashed line indicates final loop shape after many sweeps.

the final loop shape after many sweeps. The latter shows predominant capacitive charging, with the appearance of a steady-state anodic current setting in towards the voltage limit. The earlier sweeps still show an irreversible and saturable oxidation process, with the bulk of the charge transfer occurring on the first sweep.

The failure to obtain a well-defined oxidation peak and the general appearance of the first sweep indicate an electrode process that is only partially influenced by voltage. The effect of voltage is most

pronounced up to about 0.5 V and is relatively small thereafter. Since we previously observed Faradaic saturation in sweeps to 0.5 V (i.e. no further anodic currents were then observed in sweeps to 0.7 V), the results suggest that about 0.5 V is required thermodynamically to complete the process, but that a roughly voltage-independent activation, involving a time lag, is also involved.

There is some uncertainty as to the structural nature of bromine residue compounds in graphite, but there is evidence that they consist in bromine retained at graphite network defects at the interfaces between perfect and imperfect graphite layer planes [12]. At a graphite-electrolyte interface, then, one expects a relatively small number of such sites where bromine may be incorporated. It seems not unreasonable to assume that an activation process is associated either with migration to such sites or incorporation into them.

Interlamellar diffusion into the graphite does not appear to be involved. Bromide ions are not intercalated into graphite lamellae [14]; elemental bromine at moderate partial pressures seems required. The observed permanency of the above Faradaic saturation process suggests that interfacial bromide ions migrate to defect sites where they are discharged and immobilized by incorporation into the graphitic network structure.

It was of interest to see if new sites of this type could be created by interfacial stressing or deformation. For this purpose, a 'saturated' cell was compressed to various degrees with a laboratory press. Pressures insufficient to deform the cell visibly gave no change in the cyclic voltammogram. If the cell, however, was visibly plastically deformed, voltammetric sweeps with the appearance of Fig. 3 were obtained. Presumably the creation of new interfacial area resulted in new bromine incorporation sites.

Since the direct electrolytic formation of bromine residue compounds has not been reported previously, attempts were made to observe the above effects in an aqueous medium. A cell Ag, AgBr|1.0 M NH₄Br|C was made up, using a large, anodically bromided silver foil for a counter electrode and employing a nitrogen cover gas. Graphite electrodes were made by stripping several layers of graphite from the exposed graphite side of the electrolyte cell with Scotch tape and

masking the rest of the cell body. Difficulties were encountered with irreproducible impurity effects, but several such cells did indeed show voltammograms similar in appearance to Fig. 2. Thus, use of a *solid* electrolyte does not seem specifically required.

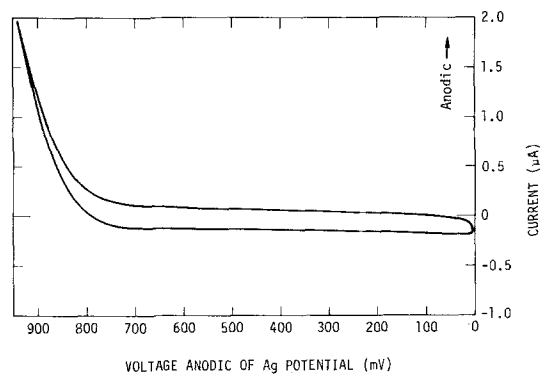


Fig. 4. Cyclic voltammograms, 'saturated' graphite electrode on AgBr, sweep rate 43 mV s⁻¹. Six sweeps.

Finally, cyclic voltammograms to 950 mV anodic of Ag|AgBr were carried out on a 'saturated' solid-electrolyte cell to observe the primary bromine discharge process. The results, shown in Fig. 4, are only qualitative because of large uncompensated resistive drop. They show a current rising smoothly to the anodic limit, with no features attributable to separate, less anodic processes. In the cell of Fig. 4, the discharge looks quite irreversible, but some cells show more clearly a slight cathodic peak of variable height. The estimated effective bromine vapor pressure at the (iR-corrected) anodic voltage limit is $\sim 3.5 \times 10^{-7}$ atm and the total anodic charge transfer per cycle (from graphical integration) is about 18 $\mu\text{coul cm}^{-2}$. Thus, an amount of bromine equivalent to a substantial fraction of a monolayer is discharged on each cycle.

From the lack of a reduction peak or anodic saturation effect, one infers rapid diffusion of the bromine into the graphite, as well as highly irreversible discharge. The low effective bromine vapor pressure at the anodic limit (i.e. the distance from the standard state bromine discharge potential) indicates probable interlamellar compound formation, which is in agreement with the assumption of rapid bromine diffusion in the graphite. Since an activation process (widening of the graphite interlamellar spacing) is known to be involved [8],

electrochemical irreversibility is to be expected.

On applying anodic voltage sweeps, then, to pressed-powder graphite electrodes on solid AgBr, two bromine discharge processes appear to occur. At about 0.5 V anodic of the Ag|AgBr potential, it becomes thermodynamically possible to saturate a small concentration of graphite surface sites with bromine, forming highly stable so-called residue compounds. An activation process appears to be involved. The bromine taken up in this manner is electroinactive and does not diffuse into the graphite. The primary bromine discharge process commences at about 0.7 V anodic of Ag|AgBr and appears to involve interlamellar compound formation and rapid bromine diffusion into the graphite.

3.3. Tetramethylammonium iodide-silver iodide double salt (TMAI) cells

Iodine discharge from $2\text{Me}_4\text{NI} \cdot 13\text{AgI}$ was of interest both because of the much higher room temperature ionic conductivity of this compound ($0.04 \Omega^{-1} \text{cm}^{-1}$) than of AgI ($\approx 10^{-4} \Omega^{-1} \text{cm}^{-1}$ for pressed powders) and because of the presence of substituted ammonium ions as an extra cationic component. Cyclic voltammetric studies in fact reveal a complex electrochemistry for iodine discharge from this electrolyte, apparently involving formation of substituted ammonium poly-iodides.

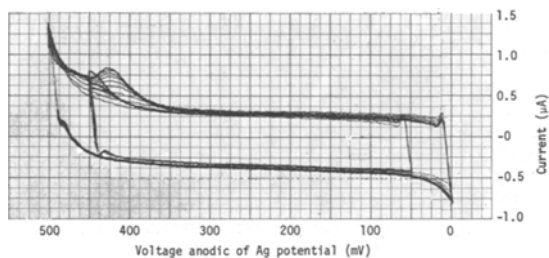


Fig. 5. Cyclic voltammogram sequence, graphite electrode on $2\text{Me}_4\text{NI} \cdot 13\text{AgI}$, sweep rate 74 mV s^{-1} . Ten sweeps. Small anodic peak at 12 mV and cathodic shoulder at 483 mV due to recorder pen bounce.

Fig. 5 shows the result of ten successive voltammetric sweep cycles at 0–500 mV anodic of the Ag potential for a TMAI cell. The small anodic peak at 12 mV and cathodic shoulder at 483 mV are due to recorder pen bounce. On the

first anodic sweep, a current upturn attributable to iodine discharge sets in at 300–350 mV, some 150 mV below that observed for AgI cells (Fig. 1). On continued sweeping, the current at the anodic voltage limit drops and simultaneously a well-defined peak develops at 425–430 mV. If the sweep cycle is stopped at this point (the voltage being returned to 0.25 V) and started again in 20 min or so, the same voltammetric sequence is repeated.

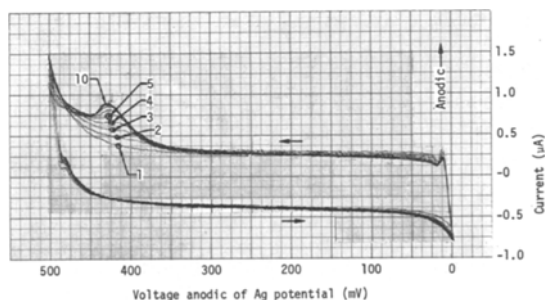


Fig. 6. Sequence of ten voltammetric cycles at 0–500 mV followed directly by three cycles at 50–450 mV for graphite electrode on $2\text{Me}_4\text{NI} \cdot 13\text{AgI}$. Sweep rate 74 mV s^{-1} .

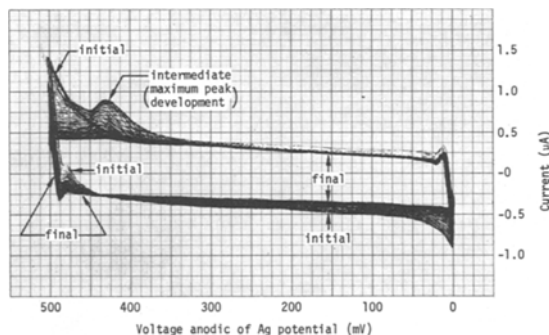


Fig. 7. Result of continuous voltammetric cycling to final capacitative loop shape for graphite electrode on $2\text{Me}_4\text{NI} \cdot 13\text{AgI}$. Sweep speed 74 mV s^{-1} . Initial anodic current trace darkened for clarity.

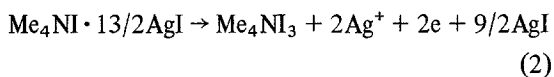
The only visual indication of a reduction process during cathodic sweeping is a current downturn towards 0 mV, commencing at 75 mV. If, during the course of sweeping, after the 428 mV peak is developed, the sweep range is narrowed to 50–450 mV, preventing the cathodic downturn, the anodic peak is then shifted to a higher voltage and its height reduced in successive sweeps. This is illustrated in Fig. 6.

Fig. 7 shows the result of continuous voltammetric cycling in the range 0–500 mV. The anodic peak first develops as described, and then *all* redox

features gradually disappear, leaving an almost purely capacitive final loop shape. The latter then becomes the permanent voltammetric cell behavior, irrespective of subsequent 'rest periods', either on or off voltage. The final loop shape serves the useful function of a reference current level for Faradaic processes and shows, for instance, that there was indeed a broad low-level reduction current in the range 0–437 mV during the cathodic voltage sweeps.

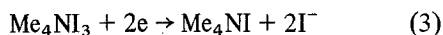
Tetramethylammonium iodide is known [15] to form at least three poly-iodides; Me_4NI_3 , Me_4NI_5 , and Me_4NI_9 . Topol [16] has measured their free energies of formation with solid-electrolyte cells. From his data, discharge of iodine as the lowest polyiodide Me_4NI_3 would reduce the thermodynamically required standard-state potential by 76 mV. Allowing for electrode-kinetic factors, resistive drop corrections and the like, we estimate that this is consistent with the reduced voltage observed for the initial anodic current upswing in Fig. 5, compared with Fig. 1.

In the first anodic sweep, then, in Figs. 5–7, we assume the Faradaic process is

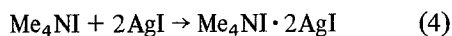


involving electrolyte decomposition and formation of the lowest polyiodide. From graphical integration of the anodic charge, using the final loop shape of Fig. 7 as the zero level for Faradaic current, we estimate that this first sweep involves about 5% of the TMAI in the interfacial electrolyte layer to the depth of one unit cell.

On cathodic sweeping, Me_4NI_3 is presumably reduced to Me_4NI

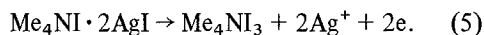


which may then simultaneously or subsequently chemically recombine with the locally available AgI to some extent. Since we do in fact observe development of a 428 mV anodic peak, we assume a new species is becoming involved in polyiodide formation. Since the only other known double salt in the Me_4NI -AgI system is $\text{Me}_4\text{NI} \cdot 2\text{AgI}$, we assume occurrence of the reaction

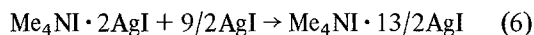


together with or subsequent to Reaction 3. Following [3], then, Me_4NI -AgI recombination to give

the original electrolyte composition is at best incomplete during voltammetric cycling, and the new species makes possible an alternate anodic electrode reaction

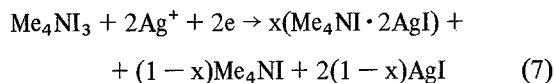


In comparing Reactions 2 and 5, we see that the latter requires less free energy by the amount of their (spontaneous) difference reaction:



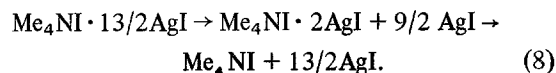
so that Reaction 5 would proceed at a lower potential, as observed. On cycling, then, $\text{Me}_4\text{NI} \cdot 2\text{AgI}$ and AgI appear to build up at the interface at the expense of $\text{Me}_4\text{NI} \cdot 13/2\text{AgI}$, with the observed voltammetric results (Fig. 5). Then, as in Fig. 6, changing the cathodic voltage limit to 50 mV during a cathodic sweep presumably results in incomplete reduction of Me_4NI_3 , resulting in less $\text{Me}_4\text{NI} \cdot 2\text{AgI}$ for the next anodic sweep.

With this reaction model, continued sweeping would involve Reaction 3 cathodically and a mixture of Reactions 2 and 5 anodically. In 'rest' periods following a limited number of sweeps, it would appear that Reaction 6 restores the initial electrolyte composition. We have, however, to explain the gradual disappearance of Faradaic activity. We postulate that the build-up of the presumed electroinactive species Me_4NI is involved; an 'alkali halide' type compound whose iodide ions would not readily be oxidized. We combine Reactions 3 and 4 in the following manner



to indicate that Reaction 4 is only partial. Then if Me_4NI is inactive electrochemically, its concentration would build up on cycling till the electrode interface becomes a mixture of Me_4NI and AgI. Both Me_4NI and $\text{Me}_4\text{NI} \cdot 2\text{AgI}$ are near-insulators at room temperature [3]. $\text{Me}_4\text{NI} \cdot 2\text{AgI}$, however, contains the necessary AgI for anodic polyiodide formation (Reaction 5), so an interfacial layer of it should be electroactive while Me_4NI is not.

On continued cycling, then, one postulates that the composition of the interfacial electrolyte layer follows the sequence



From the graphical integration measurements, it was indicated that when the 428 mV peak has developed to its maximum height, the interface consists of comparable quantities of $\text{Me}_4\text{NI} \cdot 13/2\text{AgI}$ and $\text{Me}_4\text{NI} \cdot 2\text{AgI}$, with presumably a minor amount of Me_4NI . If cycling is not continued beyond this point, it appears that recombination to the original electrolyte composition can occur. However, if appreciable amounts of Me_4NI are allowed to build up, it may then be that slow recombination of Me_4NI and AgI could permit the growth of broad interfacial patches of these two compounds, with the recombination rate continually decreasing with increasing patch size. The final voltammetric behaviour should then be that of AgI admixed with an electroinactive interface component.

A final voltammetric feature of interest is the notable cathodic current increase (downturn) in the range 0–50 mV observed in Fig. 5–7. At higher voltages, Fig. 7 shows a slow, relatively voltage-invariant cathodic process, as might be expected from the presumed low mobility of iodine and iodide ions in the electrolyte. It seems more than coincidental that a pronounced current increase occurs in a voltage range where the silver metal activity ($a_{\text{Ag}} = \exp(-FV/RT)$) becomes appreciable.

Silver ion discharge as an extra cathodic process would seem ruled out because of the absence of an anodic stripping peak on sweep reversal. Also, other work [4, 20] indicates that Ag^+ discharge on graphite from silver halides does not occur anodic of the Ag potential.

In some solid electrolytes, appreciable activity of the metallic component gives rise to a significant free electron concentration in the electrolyte [17]. In the present case, electron migration across the interface could then provide a rapid alternative process to cathodic reduction at the electrode surface. Evidence to date [3] suggests that electron concentrations in TMAI are low, even when it is equilibrated with metallic silver.

Another alternative, however, is electron injection from the electrode, as in the case of stabilized zirconia at sufficiently cathodic potentials [18, 19]. This process seems reasonable in the present case in view of the presumed thickness of electrolyte reaction layer. It would seem that some such process is indeed necessary to

explain the observed qualitative change in the trend of the cathodic voltammetric current near the Ag^+ discharge potential.

4. Summary

The room temperature halogen ion discharge characteristics of three silver halide solid electrolytes on graphite have been studied by cyclic voltammetry on pressed-powder pellet cells. Only AgI showed 'ideal' discharge characteristics (rapid, reversible; simple electrode reaction). While iodine discharge shows no chemical interaction with graphite, bromine appears to form both lamellar and residue graphitic compounds. The direct formation of residue compounds has not been previously reported, but seems the most satisfactory explanation of the effects observed. Cyclic iodine discharge and re-reduction from $2\text{Me}_4\text{NI} \cdot 13\text{AgI}$ appears to follow a complex electrochemical path involving polyiodide formation and gradual electrolyte decomposition to Me_4NI and AgI .

Acknowledgements

The author is grateful to Mr W. M. Moore for carrying out much of the experimental work, to Dr I.B. Goldberg for very helpful discussions, and to Dr B.B. Owens of Gould, Inc., for providing the $2\text{Me}_4\text{NI} \cdot 13\text{AgI}$ electrolyte.

References

- [1] See, for instance, D.O. Raleigh, *Electroanal. Chem.* **6** (1973) 87.
- [2] D.O. Raleigh, *J. Electrochem. Soc.* **121** (1974) 632.
- [3] B.B. Owens, *J. Electrochem. Soc.* **117** (1970) 1536.
- [4] M.N. Hull and A.A. Pilla, *J. Electrochem. Soc.*, **118** (1971) 72.
- [5] L.E. Topol, *Inorg. Chem.*, **7** (1968) 451.
- [6] P. Connor, J.B. Lewis, and W.J. Thomas, Proc. 5th Carbon Conf., University Park, Pa. (Pergamon Press, 1962), p. 120.
- [7] U.S. National Bureau of Standards Circular 500 (Washington 1952).
- [8] W. Rudorff, *Z. anorg. allgem. Chem.*, **245** (1941) 383; *Adv. Inorg. Chem. & Radiochem.*, **1** (1959) 224.
- [9] B. Bach, M. Bagouin, F. Bloc, and A. Herold, *Compt. Rend.* **257** (1963) 681.
- [10] G.R. Hennig, *Prog. Inorg. Chem.*, **1** (1959) 125.
- [11] G.R. Hennig, *J. Chem. Phys.*, **20** (1952) 1443.
- [12] J. Maire and J. Mering, Proc. 3rd Carbon Conf., Buffalo, N.Y., p. 337 (Pergamon Press, 1959).

-
- [13] A.R. Ubbelohde and F.A. Lewis, 'Graphite and its Crystal Compounds', p. 121 (Oxford Univ. Press, 1960).
- [14] J.M. Finn, 'Encyclopedia of Electrochemistry', pp. 151-2 (C.A. Hampel, ed.; Reinhold, N.Y., 1964).
- [15] F.D. Chattaway and G. Hoyle, *J. Chem. Soc.*, **123** (1923) 654.
- [16] L.E. Topol, *Inorg. Chem.*, **10** (1971) 736.
- [17] B. Ilshner, *J. Chem. Phys.*, **28** (1958) 1109.
- [18] R.E.W. Casselton, 'Electromotive Force Measurements in High-Temperature Systems' (C.B. Alcock, ed.), Elsevier, New York, 1968, pp. 151-7.
- [19] M. Kleitz, thesis, Grenoble (1968).
- [20] D.O. Raleigh, *J. Phys. Chem.*, **71** (1967) 1785.